29th Congress of the International Council of the Aeronautical Sciences
St. Petersburg, Russia; September 7-12, 2014

# REAL-TIME AIRCRAFT CONTINUOUS DESCENT TRAJECTORY OPTIMIZATION WITH ATC TIME CONSTRAINTS USING DIRECT COLLOCATION METHODS

**Ronald Verhoeven, National Aerospace Laboratory (NLR),** *ronald.verhoeven@nlr.nl*
**Ramon Dalmau, Technical University of Catalonia (UPC),** *ramon.dalmau@esudiant.upc.edu*
**Xavier Prats, Technical University of Catalonia (UPC),** *xavier.prats@upc.edu*
**Nico de Gelder, National Aerospace Laboratory (NLR),** *nico.de.gelder@nlr.nl*

## Abstract

*In this paper an initial implementation of a real-time aircraft trajectory optimization algorithm is presented. The aircraft trajectory for descent and approach is computed for minimum use of thrust and speed brake in support of a "green" continuous descent and approach flight operation, while complying with ATC time constraints for maintaining runway throughput and considering realistic wind conditions. The trajectory optimizer forms an important part of a new integrated, planning and guidance concept named TEMO (Time and Energy Managed Operations) developed in the Systems for Green Operations (SGO) Clean Sky EU-program. It is compared with a typical A320 Flight Management System (FMS) showing improvements regarding time adherence performance and environmental impact.*

## 1 Introduction

The expected growth in air traffic [1], combined with an increased public concern for the environment and increased oil-prices, have forced the aviation community to rethink the current air traffic system design. The current air traffic system operates close to its capacity limits and is expected to lead to increased delays if traffic levels grow even further [2]. Both in the United States [3] and Europe [4], research projects have been initiated to develop the future Air Transportation System (ATS) to address capacity, environmental, safety and economic issues.

To address the environmental issues during descent and approach, a novel Continuous Descent Operations (CDO) concept [5], named Time and Energy Managed Operations (TEMO) [6][7], has been developed.

It uses energy principles to reduce fuel burn, gaseous emissions and noise nuisance whilst maintaining runway capacity. Different from other CDO concepts, TEMO optimizes the descent by using energy management to achieve a continuous engine-idle descent while satisfying time constraints. As such, TEMO uses a Required Time of Arrival (RTA) at the Initial Approach Fix and subsequently an Assigned Spacing Goal (ASG) at the Final Approach Point (FAP)[8] to facilitate flow management and arrival spacing.

Given a sequence of phases during descent and approach as defined in the TEMO concept of operations, a set of path constraints and boundary conditions is defined. Together with the given meteorological conditions, predefined optimality criteria, an accurate initial guess and current aircraft state, a multiphase optimal control problem is solved in real-time using direct collocation methods. Important optimizer performance accelerators are the use of automatic differentiation techniques and smooth curve fittings to model aircraft performance.

The real-time on-board re-planning of the remaining descent trajectory during the descent (given the current state and a comprehensive set of operational constraints), triggered by energy and/or time errors is considered novel, both in concept as well as in implementation. This paper discusses the algorithm implementation and performance aspects, showing some example results of a realistic descent trajectory, which are compared with a typical FMS, as can be found in an Airbus A320, for instance.

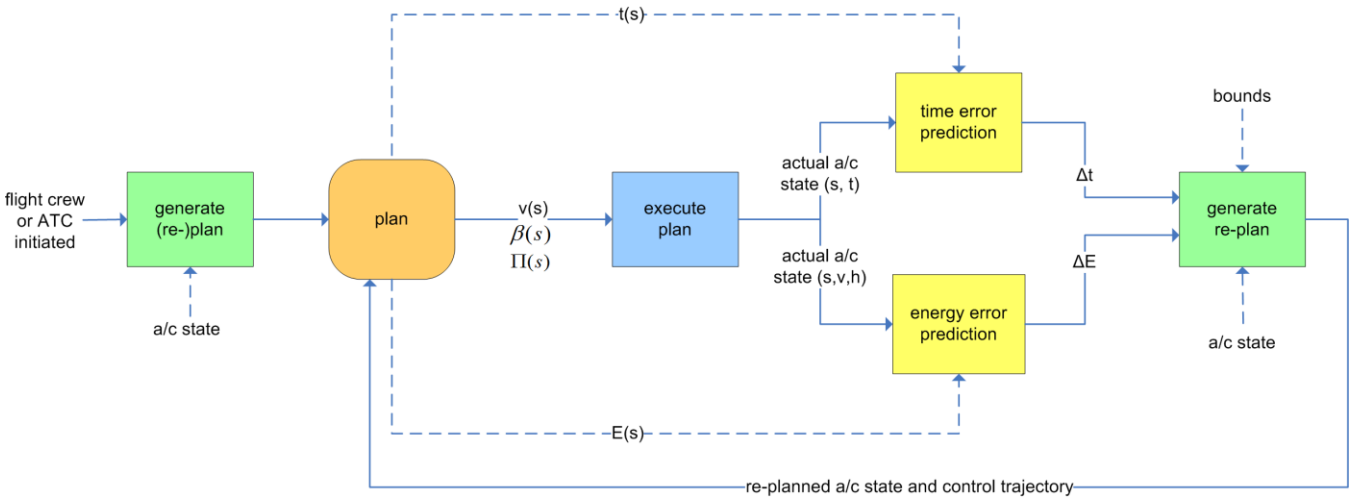


**Fig. 1 Trajectory optimizer block diagram**

## 2 Time and Energy managed operations

During the cruise phase (before entering the descent phase at Top of Descent – TOD) of a flight an optimal descent trajectory is planned by the Flight Management System (FMS) of the aircraft. The descent trajectory may have to comply with one or more constraints. Typical types of constraints are altitude, speed and/or time constraints. In today's standard the FMS will calculate and freeze the initial idle descent path before TOD and the aircraft will be guided along that path, initially with idle thrust and "path on elevator".

In the new TEMO concept, the trajectory is optimized with respect to predefined objectives (e.g. fuel, $NO_x$, $CO_x$, noise,...). The planned descent trajectory is executed in "speed on elevator" mode. This implies that the aircraft may deviate from the planned altitude profile while maintaining the planned speed using the aircraft elevators.

Associated with the planned trajectory, maximum allowable energy and time deviations are defined along the descent. If after entering the descent phase of a flight the maximum allowable energy and/or time boundary is exceeded, the current planned descent trajectory is updated with an (new) optimized descent trajectory, given the current state, applicable constraints and optimality objectives (see Fig. 1).

To calculate the earliest/latest feasible arrival times at predefined points of the descent the same TEMO optimization functionality is used. In these cases, the objective function is changed to minimize/maximize the time of arrival at the waypoint subject to a time constraint. This enables the flight crew and/or on-board systems to evaluate the feasibility of ATC imposed constraints before the TEMO optimization function is deployed. In particular it is expected that ATC imposed time constraints are defined at the IAF and either the FAP or Runway Threshold (RTH), but the algorithm is generic enough to consider time constraints at any given waypoint.

### 2.1 Trajectory optimization

The optimization of an aircraft trajectory, as a 4 dimensional continuum, is a multi-phase constrained optimal control problem. These kinds of problems are not easy to solve, especially when nonlinear functions appear in the definition of the optimization objective and/or the constraints. The problem presented in this paper is solved by direct collocation methods, where the original infinite and continuous problem is discretized and transformed to a nonlinear programming (NLP) problem with a finite set of variables [9].

Several collocation strategies are found in the literature, like for instance Euler, Trapezoidal, Runge-Kutta, Hermite-Simpson,

Pseudospectral, etc. [10] In this paper a Trapezoidal collocation scheme has been used, since it has shown a good compromise between the achieved trajectory accuracy and algorithm execution time.

In this paper, the state ($\boldsymbol{x}$) and control ($\boldsymbol{u}$) vectors are defined as:

$$\boldsymbol{x} = [v_a, \gamma_a, s, h, m]^T;\ \boldsymbol{u} = [\Pi, \beta, n_z]^T \quad (1)$$

where $v_a$ is the true airspeed, $\gamma_a$ is the aerodynamic flight path angle, $s$ is the along path distance (from the runway threshold), $h$ is the geometric altitude, $m$ the mass of the aircraft, $\Pi \in [0,1]$ the engine throttle position, $\beta \in [0,1]$ the speedbrakes lever position and $n_z$ the vertical load factor.

The goal for solving the optimal control problem is to find the *best* control vector function over the time period $[t_0, t_f]$ that minimizes a given performance index (or cost function). In this paper, we use a compound function considering the total fuel burnt and the time integration of the speed brakes usage:

$$J = \int_{t_0}^{t_f} (FF + \beta)\mathrm{d}\tau \quad (2)$$

where $FF$ is the fuel flow depending on the throttle setting, speed and atmospheric conditions.

## 2.2 Optimization constraints

In order to guarantee a feasible and acceptable trajectory, as a result of this optimization process, several constraints must be considered. In particular, the *dynamics of the system* (state vector), which in this paper are modeled with a typical nonlinear point-mass model of the aircraft. Thus, the aircraft is assumed as a rigid-body moving over a flat nonrotating earth with constant gravity acceleration ($g$) and where angle of attack and sideslip angles are neglected. The effect of wind and wind shear are only considered in the horizontal plane and it is assumed that they can change only as a function of the along path distance and altitude. Thus, vertical wind components and temporal wind variations are neglected.

Taking all these considerations into account, the aircraft dynamics, expressed in the air reference frame are generally given by:

$$\begin{aligned} \dot{v}_a &= \frac{T - D}{m} - g\sin\gamma_a - \dot{W}_v \\ \dot{\gamma}_a &= \frac{g}{v_a}\left[n_z\cos\phi - \cos\gamma_a + \frac{\dot{W}_\gamma}{g}\right] \\ \dot{s} &= \sqrt{v_a^2\cos^2\gamma_a - W_x^2} + W_s \\ \dot{h} &= v_a\sin\gamma_a \\ \dot{m} &= -FF \end{aligned} \quad (3)$$

where $T$ and $D$ are respectively the Thrust and Drag forces acting on the aircraft, which are modeled as a function of state and control vector variables by using accurate performance values . Since the horizontal path of the aircraft is known beforehand, the bank angle $\phi$ can be computed for each turn as a function of the state variables. $W_s$ and $W_x$ are the along track and crosstrack wind components, respectively, while the wind shear components $\dot{W}_v$ and $\dot{W}_\gamma$ can be modeled as functions of the along track and crosstrack wind variations and the state variables [7].

Flight operational restrictions are also modeled as optimization constraints. For the whole trajectory, the load factor is bounded by upper and lower constraints, considering passenger comfort criteria. On the other hand, airspeed and altitude are also subject to several constraints, but they change all along the trajectory. Thus, the trajectory is split in several phases where a particular set of constraints is defined for each of them.

The TEMO descent presented in this paper is split into 14 different phases that consider, for instance, different flap/slat configurations, constant velocity or deceleration segments (which can be in terms of Mach number or calibrated airspeed), fixed vertical path segments (imposed when the aircraft is following the Instrument Landing System glide slope), etc. The definition of the different phases and the particular details for each set of constraints can be found in [7].

## 3. Implementation aspects

Fig. 2 shows a generic architecture of a trajectory optimizer. The nominal plan is constructed by backwards integration given the runway threshold as starting point, control trajectory, path constraints and boundary conditions (but without considering time constraints). Preferably, a variable step-size integration method should be chosen such as the Runge-Kutta-Fehlberg method [12]. The output trajectory can be used as initial flight plan and as first guess for the optimizer.

Then, the trajectory is optimized under the given optimality criteria subject to path constraints and boundary conditions and margins using a Non-Linear Problem (NLP) solver. Anticipating the time needed to generate an optimized trajectory, the initial start point of the optimized trajectory must be chosen ahead of the current aircraft position, considering current time & state deviations and the active plan. Outputs are a control and state trajectory encompassing the optimized plan.

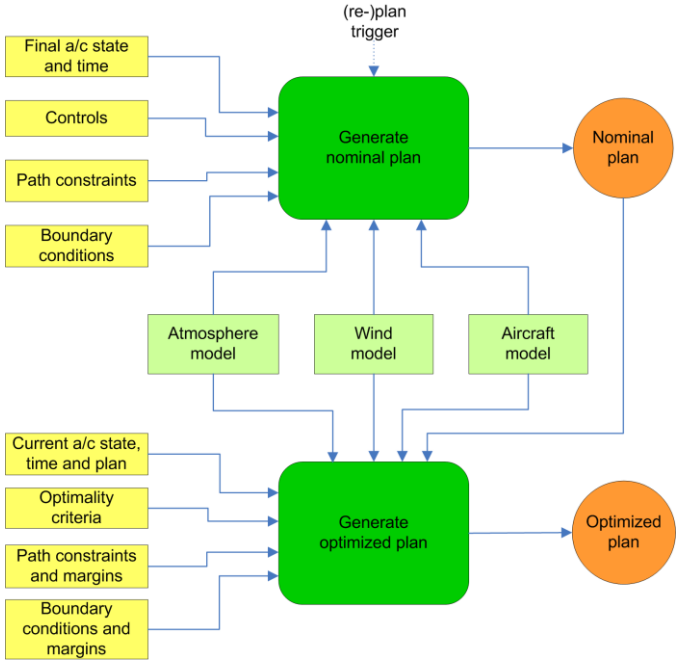


**Fig. 2 Generic architecture of a trajectory optimizer**

Fig 3. shows the architecture of the TEMO implementation, which was developed aiming at Technology Readiness Level (TRL) 5. Note that although in Fig 3. TEMO is drawn outside the Flight Management System (FMS), in general, trajectory optimization is a function to be performed by the aircraft FMS.

The General Algebraic Modeling System (GAMS) [13] is used as platform for solving the optimalisation problem. The NLP solver chosen is CONOPT [14], a commercial solver for large-scale nonlinear optimization. Gradients and Hessian are automatically provided by GAMS, using its automatic differentiation engine. In between the FMS and GAMS, a C++ layer is implemented which sets up the multi-phase optimization problem and processes the results obtained by the NLP solver using the GDX API of GAMS. In this layer also the nominal trajectory is calculated which is used as first guess for the optimizer. The trajectory is optimized along a fixed route which may consist of track to a fix and fixed radius legs. A fly-by turn is used to transition from one track to fix leg to another track to fix leg. The final part of the descent trajectory is the ILS, the ILS glide slope (g/s) takes the earth curvature into account. Also the transition level from STD to QNH altimeter-setting is considered in the generated altitude profile. The aircraft performance is modelled by using 1D and 2D polynomial approximations of available tabular performance data.

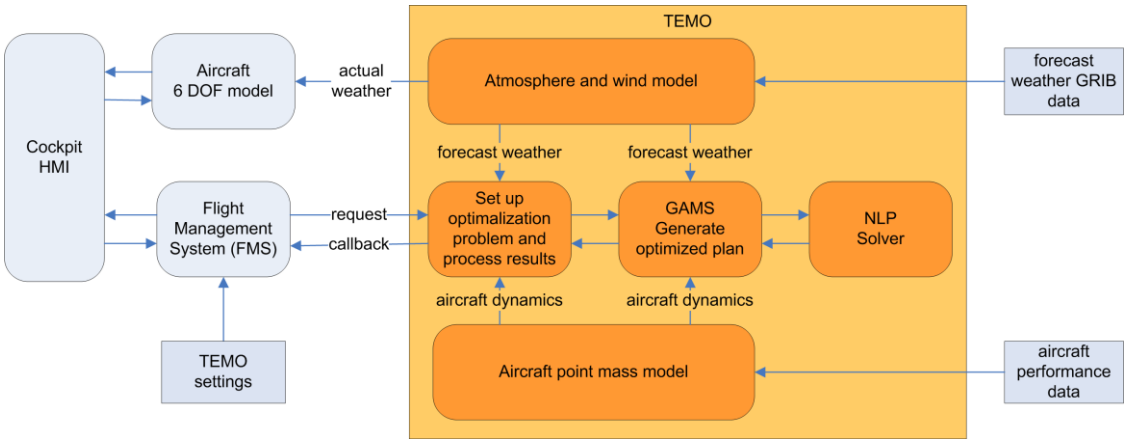


**Fig. 3 Overview of the TEMO implementation**

The forecasted pressure, temperature and wind data obtained from GRIB formatted files are modelled using splines in the atmosphere and wind model. Actual weather is simulated by adding an offset on the forecasted weather data.

## 4. Results

A realistic descent of an Airbus A320, from cruise at FL360 to Eelde airport, in the Netherlands, has been simulated to produce some illustrative results. The REKKEN1G standard instrument arrival, followed by the TOLKO1G RNAV-ILS approach, has been flown (see Fig. 4) [11].

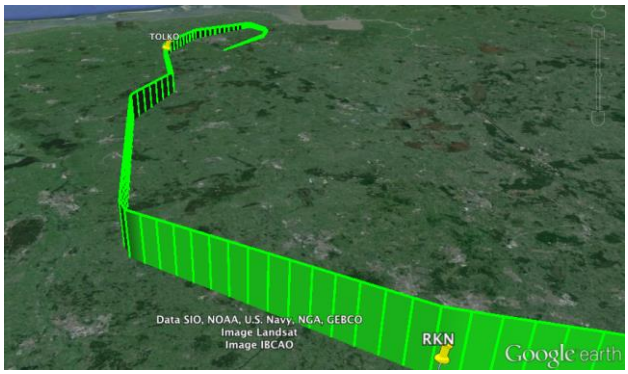


**Fig. 4 Arrival and approach procedure simulated to Eelde airport.**

Recorded weather data, from the 10th of April 2012 over the Netherlands, have been used to initialize the weather component. Two cases will be considered in this section: a hypothetical scenario with no wind prediction errors, and a simulation in which forecast winds are overestimated by 15 kt.

The result of the initial TEMO plan produces an optimal thrust idle descent with no speed brake usage. Well before the TOD, it is assumed that ATC requests an RTA over the Final Approach Point (FAP), which is 5 minutes before the originally planned time over that point. This is an operational unlikely scenario but a stressing test for the TEMO algorithm. Fig. 4 shows the optimal solution for this re-planned trajectory.

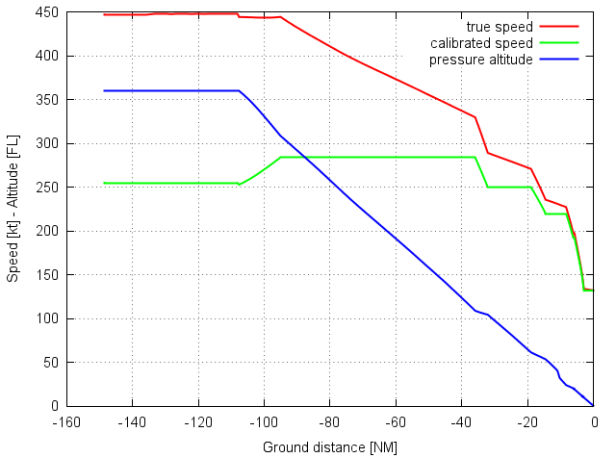


**Fig. 5 Optimal solution for the re-planned trajectory.**

This re-plan considers a constant pressure altitude and Mach cruise phase before reaching the TOD. The optimal TOD according to the cost function, see equation (2), and considering the RTA is located approximately at 110 NM from the runway threshold; well ahead the initial planned TOD at 122 NM. This shift of the TOD is caused by the higher speed profile required by the RTA. The changes in true airspeed shown in Fig. 5 during the cruise

phase are caused by variations of temperature predictions along the flight path. When reaching the TOD, a phase with constant descent Mach starts, followed by a phase having a constant CAS. At the IAF TOLKO (33 NM from the runway threshold) and at waypoint EH740 (15 NM from the runway threshold) CAS is constrained, respectively, to 250 kt and 220 kt. Therefore, constant deceleration phases are used in order to comply with these operational constraints. Another deceleration phase is introduced to decelerate towards the green dot speed, at which the aircraft starts configuring slats (config 1) while descending. The re-plan assumes that the ILS glide slope is intercepted at the FAP with S speed. When on the glide path, the aircraft will descend and decelerate while configuring in order to reach the final approach speed at 1000 ft in landing configuration.

Fig. 6 and Fig. 7 show, respectively, the energy and time deviations with respect to the plan, as a function of the along path distance of the TEMO operation from the initial aircraft position to the ILS glide slope interception, thereafter re-planning is disabled. The error margins that determine whether a re-plan is initiated are shown in Table 1. These error margins are defined symmetrically.

**Table 1 TEMO error boundaries**

| Error type | TOD | IAF | Runway threshold |
|---|---|---|---|
| Time [s] | ±20 | ±10 | ±5 |
| Energy [ft] | ±500 | ±300 | ±100 |

For the simulation without wind prediction errors (i.e. the wind considered during the re-planning process matches the actual wind) energy and time errors remain within the defined boundaries and no additional re-plan is triggered. Therefore, the aircraft is able to comply with the RTA following the first re-plan with no significant time and energy errors. The small energy and time errors observed, respectively, in Fig. 6 and Fig. 7 are caused by inaccuracies in the TEMO models (mainly with aircraft performance) and the errors due to the flight guidance implementation.

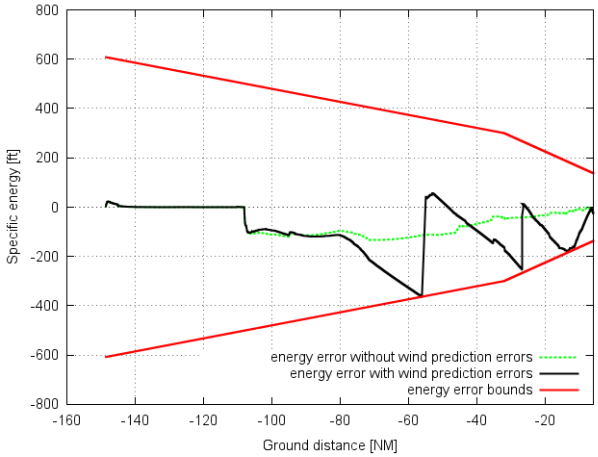


**Fig. 6 TEMO energy error with and without wind prediction errors**

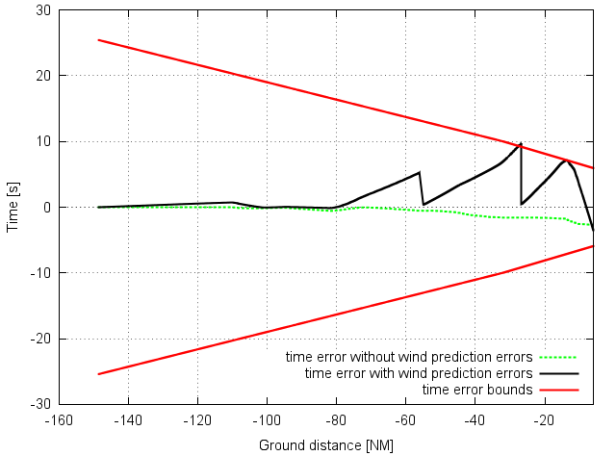


Fig. 7 TEMO time error with and without wind prediction errors

For the simulation with wind prediction errors two additional re-plans are triggered during the descent. From the initial aircraft position to approximately 80 NM from the runway threshold, the along path wind component is small and wind speed prediction errors do not cause significant energy or time errors. When reaching EH522 the aircraft track changes from 309° to 0° and the along path wind component error becomes a factor. Time and energy errors start to increase in absolute value up to the point the energy error reaches the boundary and triggers a second re-plan at approximately 55 NM from the runway threshold.

When the second re-plan becomes active energy and time errors are close to zero since the aircraft is following the newly planned path,

speed and time. As the second re-plan is computed with the initial wind prediction time and energy errors increase again.

The third re-plan is triggered by an excessive time deviation crossing the boundary at 28 NM from the runway threshold (just after passing the IAF). While flying the third re-plan the energy and time errors increase again and are about to reach both time and energy error boundaries at EH741. *Fortunately*, at EH741 the track almost changes 180°, and the along path wind component error works in favor of the energy and time deviations: both time and errors start to decrease and the aircraft intercepts the ILS g/s with almost no time and energy errors.

Fig. 9 shows the controls for the simulation in which forecast winds are overestimated by 15 kt. The executed descent keeps thrust at idle from the TOD down to the ILS g/s interception but requires speed-brakes to comply with the RTA.

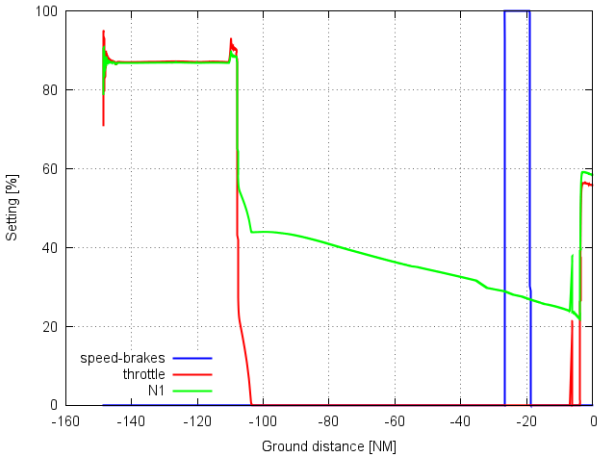


**Fig. 9 Thrust and speed brake usage during the simulation**

The scenario with an RTA used in the TEMO simulations has also been simulated with a typical FMS behavior. In order to comply with the RTA, the FMS iterates with the cost index until the RTA is matched. Fig. 10 and 11 show, respectively, the speed and time errors, as a function of the along path distance of the flight operation.

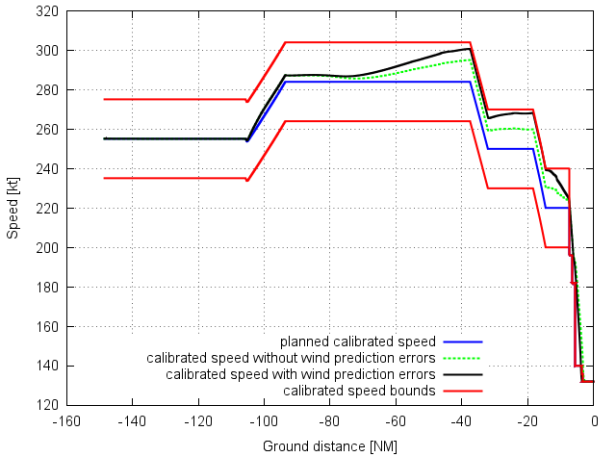


**Fig. 10 FMS speed profile with and without wind prediction errors**

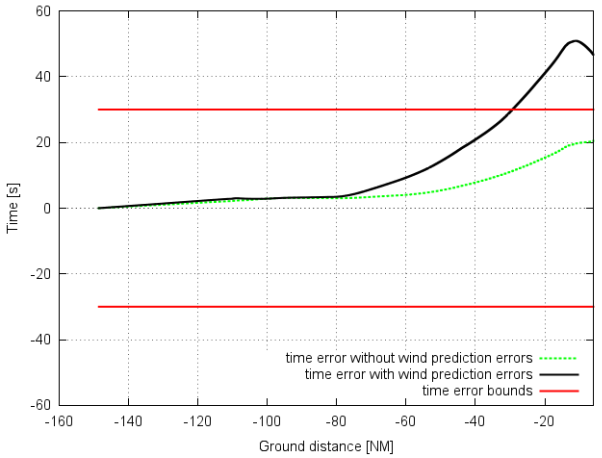


**Fig. 11 FMS time error with and without wind prediction errors**

When the speed is managed and the vertical deviation from the planned path is less than 50 ft, a target speed range defines acceptable speed variations around the nominal descent planned speed (± 20 kt). The vertical guidance will modify the speed between this range in order to nullify vertical path errors.

The wind prediction is only entered at 5 altitudes. Between these altitudes a linear interpolation is used and some deviations can be expected. In addition, the small temperature and pressure deviations from the ISA profile considered during the re-plan computation are also contributing to the calibrated airspeed deviations from the plan shown in Fig 10. The time constraint is considered missed if the time error is greater than 30 seconds. According to Fig. 11 the aircraft is fulfilling the RTA with

the 30 seconds criteria in absence of wind prediction errors.

For the simulation with wind prediction errors, CAS deviations needed to follow the vertical path are greater. As in the TEMO descent, along path wind component error starts to become significant at 80 NM from the runway threshold. Time and CAS deviations from the plan grow until EH741 is reached and the along path wind component error sign changes. In this case, the FAP is reached with more than 30 seconds error and the RTA is missed considering the 30 seconds criteria. In this simulation the FMS does not re-plan during the descent.

In this paper, noise, total fuel burned and time error with respect the RTA have been chosen as performance indicators to provide a first preliminary result of the TEMO concept benefits. Figs. 12 and 13 show, respectively, the noise footprints as a function of the along path distance for both scenarios. The noise foot prints are calculated using the noise model as described in [1].

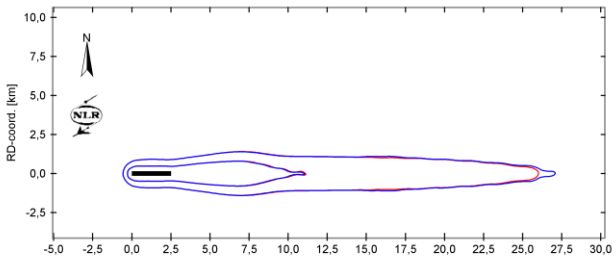


**Fig. 12 Noise footprint comparison for the scenarios without wind prediction errors (blue FMS, red TEMO)**

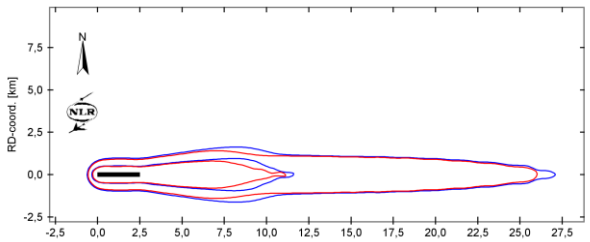


**Fig. 13 Noise footprint comparison for the scenarios with wind prediction errors (blue FMS, red TEMO)**.

The normalized sound exposure level (SEL) contour areas, the normalized total fuel burned and the time errors at the FAP are presented in Table 2 for both considered scenarios.

**Table 2 Normalized performance indicators comparison between TEMO and FMS operations**

| Performance indicator | Without wind prediction errors | | With prediction errors | |
|---|---|---|---|---|
| | FMS | TEMO | FMS | TEMO |
| Total fuel burned (%) | 100.0 | 98.3 | 105.4 | 103.9 |
| SEL contour area (%) | 100.0 | 90.5 | 100.0 | 92.9 |
| Time error [s] | 20.0 | -2.9 | 46.8 | -3.4 |

## Conclusions

Results demonstrate that the TEMO implementation is capable of guiding the aircraft along a planned TEMO trajectory complying with an RTA, even if significant wind prediction errors are present. For a same scenario, a typical FMS without replanning capabilities during descent, would miss the RTA.

Moreover, preliminary results show noise benefits in the order of 7-9% and fuel benefits in the order of 1.5% for the TEMO operations. The preliminary results also illustrate the importance of accurate wind predictions, in particular for total fuel burned. In case FMS with re-planning capabilities is considered, increased noise and fuel benefits may be expected.

## Acknowledgment

The research leading to these results received funding from the European Union's Seventh Framework Programme (FP7/2007-2013) through the Clean Sky Joint Technology Initiative under Grant Agreements nos. CSJU-GAMSGO-2008-001 and CS-GA-2013-323495 (FASTOP project).

The authors acknowledge the contributions and effort of Florent Birling, Isidro Bas, Santi Vilardaga and Roger Isanta of the FASTOP consortium with developed the TRL-5 version of the weather model and trajectory optimizer. Furthermore, the work and contributions of Frank Bussink, Michel van Eenige, Jaap Groeneweg, Bart Heesbeen, Roel

Hogenhuis, Adri Marsman, Wilfred Rouwhorst, Michiel Valens (all NLR), and Paul de Jong (PhD former student of TU-Delft) are acknowledged.

## References

[1] EUROCONTROL, *Long-Term Forecast: IFR Flight Movements 2010-2030*, Tech. Rep. CND/STATFOR Doc415, EUROCONTROL, December 2010.

[2] SESAR, *Air Transport Framework: The Current Situation*, Tech. Rep. SESAR TR DLM-0602-001-03-00, EUROCONTROL, July 2006.

[3] NextGen Office, *FAA's NextGen Implementation Plan 2012*, Tech. Rep., FAA, 800 Independence Avenue, Washington, DC, March 2012.

[4] SESAR, *European ATM Master Plan*, Tech. Rep. Edition 2, EUROCONTROL, October 2012, SESAR JU & SESAR Work Package C and Partners.

[5] ICAO, *Continuous Descent Operations (CDO) Manual - Doc 9931 AN/476*, International Civil Aviation Organization, Montreal, Canada, 2010.

[6] De Jong, P. M. A., De Gelder, N., Bussink, F. J. L., Verhoeven, R. P. M., Kohrs, R., and Mulder, M., *Time and Energy Management during Descent and Approach for Aircraft: A Batch-Simulation Study*, Journal of Aircraft, 2013

[7] Prats, X., Pérez-Batlle, M., Barrado, C., Vilardaga, S., Bas, I., Birling, F., Verhoeven, R., Marsman, A., *Enhancement of a time and energy management algorithm for continuous decent operations*, in Proceedings of the Aviation Technology, Integration and Operations (ATIO) conference. June 2014.

[8] Abbot, T. S., *A Brief History of Airborne Self-Spacing Concepts*, Contractor Report NASA/CR–2009-215695, National Aeronautics and Space Administration, Langley Research Center, Hampton, Virginia 23681-2199, February 2009.

[9] Betts, J. T. and Cramer, E. J., *Application of direct transcription to commercial aircraft trajectory optimization*, Journal of Guidance, Control and Dynamics, 18(1), pp. 151-159. Jan-Feb 1995.

[10] Betts, J. T. *Practical methods for optimal control and estimation using nonlinear programming.* Advances in Design and Control SIAM. 2nd ed. 2010

[11] Air Traffic Control The Netherlands. *Aeronautical Information Publications (AIP)* – Part AD-EHGG.

[12] Fehlberg, E., *Low-order classical Runge-Kutta formulas with step size control and their application to some heat transfer problems*, NASA Technical Report 315, 1969

[13] General Algebraic Modeling System (GAMS), http://www.gams.com

[14] CONOPT, http://www.conopt.com

[15] van der Wal, H.M.M, Vogel P., en Wubben, F.J.M., *Voorschrift voor de berekening van de $L_{den}$ en $L_{night}$ geluidbelasting in dB(A) ten gevolge van vliegverkeer van en naar de luchthaven Schiphol*, NLR-CR-2001-372-PT-1, July 2001 (in Dutch).

## Copyright Statement